ACS Catalysis

Letter

pubs.acs.org/acscatalysis

Pt−Ni Nanoparticle-Stacking Thin Film: Highly Active Electrocatalysts for Oxygen Reduction Reaction

Naoto Todoroki,* Takashi Kato, Takehiro Hayashi, Shuntaro Takahashi, and Toshimasa Wadayama

Graduate School of Environmental Studies, Tohoku University, Sendai 980-8579, Japan

Supporting Information

ABSTRACT: A novel nanoparticle-stacking thin film (NPSTF) of Pt−Ni alloy for highly active oxygen reduction reaction (ORR) electrocatalyst was synthesized. The Pt mass activity of the synthesized Pt−Ni NPSTF were 10-fold higher than commercial carbon-supported Pt catalysts. The remarkable ORR activity enhancement of the Pt−Ni NPSTF was attributed to the modified electronic properties of the surface Pt-enriched layers induced by underlying Ni atoms and to the increased active surface area achieved by stacking of Pt−Ni nanoparticles.

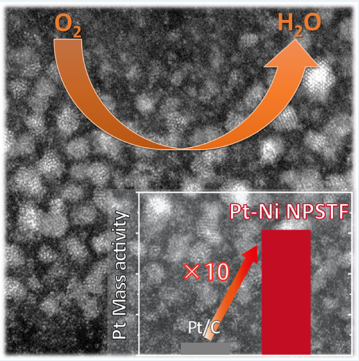

KEYWORDS: *thin film catalysts, oxygen reduction reaction, Pt-based alloys, arc plasma deposition, proton exchange membrane fuel cell*

Fuel cells are one of the key technologies to replace current fossil-fuel-based energy systems. In particular, proton exchange membrane fuel cells (PEMFCs) have been extensively studied for use as a power source in fuel cell vehicles (FCVs). Highly active and cost-effective cathode electrocatalysts for the oxygen reduction reaction (ORR) are needed to facilitate the commercialization of FCVs because of the scarcity of platinum. Over the past decade, Pt−M alloy nanoparticles (NPs) (where M is typically a 3d transition metal such as Ni, Co, or Fe)[1,2] and Pt-monolayer core−shell NPs[3,4] have been widely studied because of their enhanced ORR activities and reduced Pt loadings. However, catalysts' structures with metal (alloy) NPs on carbon supports have serious drawbacks, including agglomeration and dropout of the NPs; furthermore, the carbon supports tend to corrode under typical PEMFC operating conditions.[5]

Considering the aforementioned drawbacks of carbon-supported NP catalysts, meso- or nanostructured thin films are attracting extensive attention as effective structures for ORR catalysts.[6−8] Such thin-film catalysts possess advantages with respect to both specific activity and structural stability.[9] Furthermore, the thin-film structures of such catalysts can potentially improve the catalyst utilization rate. In the case of Pt/C catalysts, the ORR does not always proceed on all of the Pt NPs surfaces because of the diffusion limits of the reactive species (H^+ and O_2) in PEM stacks. However, the thin-film structures enable the reactants to access the catalyst surface more effectively.[10] To date, magnetron sputtering and electrochemical deposition have been used to prepare thin film catalysts.[8,11] The alloy compositions and nanoscale roughness of the thin-film catalysts determine their ORR properties. However, detailed synthesis conditions for practical ORR catalysts have yet to be further elucidated. For example, thickness of the previous reported thin film catalysts whose Pt loading per electrode geometric surface areas is higher than that of carbon-supported NP catalysts is 20−100 nm.[8] As a result, the Pt mass activities of such thin-film catalysts are much lower than those of recently reported highly active Pt/C and Pt−M/C catalysts.[12]

In this letter, we report a novel synthesis of Pt−Ni thin-film ORR catalysts on highly oriented pyrolytic graphite (HOPG) supports. First, synchronous arc plasma deposition (APD) of Pt and Ni was used to prepare the Pt−Ni thin films. The APD method can generate nanometer-sized metal particles via an arc discharge incident on the target metals; this approach enables us to fabricate much thinner films than those prepared by magnetron sputtering. We subsequently used electrochemical dealloying to dissolve excess Ni from the APD-prepared Pt−Ni thin films in 0.1 M $HClO_4$ solution. The nanostructures of the Pt−Ni catalysts obtained via the aforementioned procedure were strongly dependent on the composition of the pristine alloy. In particular, a 2−3 nm-sized Pt−Ni nanoparticle-stacking thin film (NPSTF) structure was achieved for the APD-prepared Pt_2Ni_8 thin film after the dealloying process; the Pt mass activity of the Pt−Ni NPSTF is 10-fold greater than that of typical commercial Pt/C catalysts. On the basis of the obtained results, we propose a novel synthesis method for

Received: November 6, 2014
Revised: February 28, 2015
Published: March 3, 2015

DOI: 10.1021/acscatal.5b00065
ACS Catal. 2015, 5, 2209−2212

preparing highly active Pt−Ni ORR catalysts with extremely low Pt loadings.

For the synthesis of Pt−Ni NPSTF, Pt−Ni alloy thin films were first prepared on the HOPG substrate using synchronous APD depositions of Pt and Ni. The synchronous APD system is schematically shown in Figure 1; the system incorporated two

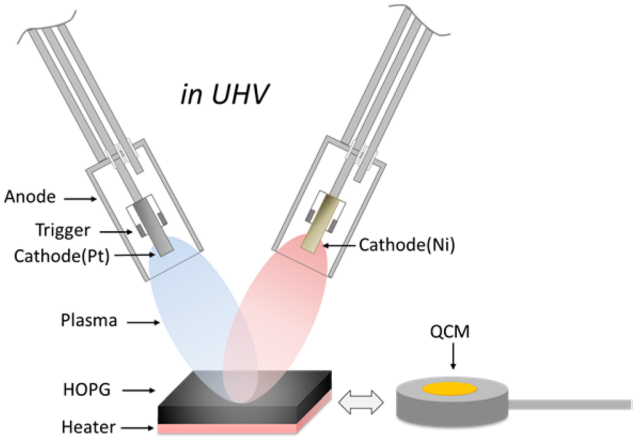

Figure 1. Schematic of the arc-plasma deposition of Pt−Ni thin films.

APD sources and a quartz crystal microbalance (QCM). Pt−Ni alloy compositions were controlled by fixing the Pt arc voltage to 100 V and adjusting that of Ni from 150 to 180 V. Table 1

Table 1. Estimated Deposition Mass (QCM) and Alloy Compositions (XPS) of APD-Prepared Pt−Ni Alloy Thin Films

	deposited mass (μg/cm^2-HOPG)			
arc voltages (V)	Pt	Ni	Pt + Ni	as-made alloy composition
Pt 100, Ni 150	0.18	0.10	0.28	Pt_4Ni_6
Pt 100, Ni 180	0.18	0.19	0.37	Pt_2Ni_8

summarizes the amounts of Pt and Ni deposited and the alloy compositions of the as-prepared Pt−Ni thin films, as estimated from Pt (4f) and Ni (2p) core-level band intensities measured by X-ray photoelectron spectroscopy (XPS). The synchronous atomic ratios of the Pt−Ni alloy thin films prepared at Ni arc voltages of 150 and 180 V were estimated to be Pt_4Ni_6 and Pt_2Ni_8, respectively.

The films were subsequently electrochemically dealloyed via potential cycling. When Pt-based alloy nanoparticles are subjected to a potential cycling pretreatment in an acidic electrolyte, less-noble alloying elements (M) are known to undergo selective dissolution, thereby forming a Pt-enriched outermost surface layer—the so-called Pt-skin (electrochemical dealloying).[13] The Pt-skin exhibits enhanced ORR activity, which can be explained on the basis of electronic (ligand) and strain effects induced by the underlying Pt−M alloys.[14] Figure 2a shows cyclic voltammograms at the first cycle for the as-prepared APD Pt−Ni thin films. Anodic currents corresponding to dissolution of Ni atoms[15] emerged in the voltammograms of both the Pt_4Ni_6 and Pt_2Ni_8; the total charge of the dissolution current strongly depended on the alloy composition. Energy-dispersive X-ray spectroscopy (EDX) showed that the alloy compositions of Pt_4Ni_6 and Pt_2Ni_8 after the dealloying process were both approximately Pt_7Ni_3.

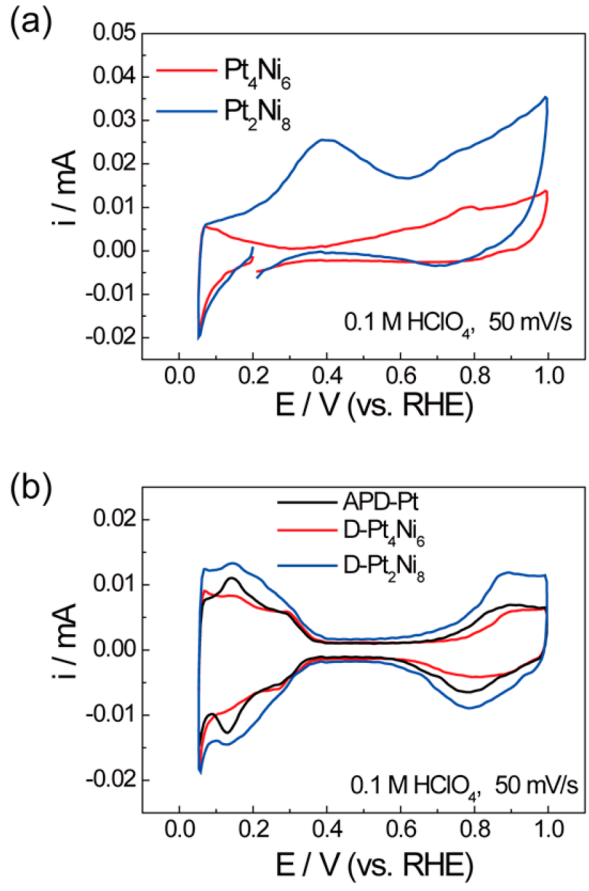

Figure 2. (a) Cyclic voltammograms at the first cycle for Pt_4Ni_6 and Pt_2Ni_8. (b) Cyclic voltammograms for D-Pt_4Ni_6, D-Pt_2Ni_8, and APD-Pt.

Figure 2b shows the cyclic voltammograms for dealloyed Pt−Ni thin films (D-Pt_xNi_{1-x}) and APD-prepared Pt (APD-Pt) as a reference material. The voltammogram for the APD-Pt corresponds well to previously reported voltammograms for Pt/C catalysts.[16] However, the voltammogram for D-Pt_4Ni_6 shows negative and positive potential shifts of the hydrogen-related (0.05−0.35 V) and hydroxyl-related (above 0.6 V) regions, respectively, relative to the potentials for APD-Pt. Such potential shifts are typical in voltammograms of highly ORR-active Pt−M(111) single-crystal surfaces.[17−20] Therefore, the results shown in Figure 2b suggest that a Pt-skin-like surface is generated upon dealloying of the Pt_4Ni_6 thin film (D-Pt_4Ni_6) through selective dissolution of the Ni atoms. In contrast, the voltammogram for the D-Pt_2Ni_8 exhibits marked extensions of both the hydrogen- and hydroxyl-related features. The result suggests that the electrochemically active surface area (ECSA) of the Pt_2Ni_8 was expanded by the dealloying process.

Figure 3a shows linear-sweep voltammograms for the ORR of the D-Pt_xNi_{1-x} and the APD-Pt recorded in O_2-saturated 0.1 M $HClO_4$ at 1600 rpm. The results indicate that the half-wave potential for the ORR at the D-Pt_4Ni_6 and D-Pt_2Ni_8 shifted to higher potentials by 15 and 30 mV, respectively, relative to that for the APD-Pt, indicating that the ORR activities increased with increasing Ni composition. Evaluation of the specific ORR activities on the basis of hydrogen adsorption charges of the Pt−M alloys is known to overestimate the activities.[21] In this study, therefore, the Pt-mass ORR activities were estimated from the deposition mass thickness of Pt and from kinetically

DOI: 10.1021/acscatal.5b00065
ACS Catal. 2015, 5, 2209−2212

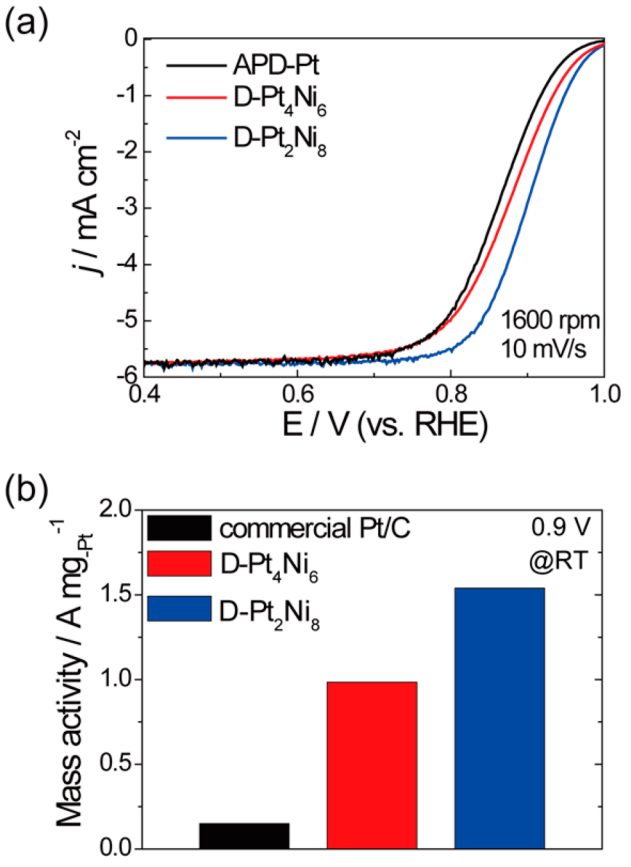

Figure 3. (a) Linear-sweep voltammograms for the ORR of D-Pt_4Ni_6, D-Pt_2Ni_8, and APD-Pt. (b) Pt-mass activities for D-Pt_4Ni_6, D-Pt_2Ni_8 and commercial Pt/C (adapted from ref 11).

controlled currents (i_k) at 0.9 V; the estimated ORR activities are summarized in Figure 3b. For comparison, the typical Pt mass activity 0.15 A/mg_{-Pt} for the commercial Pt/C catalysts (e.g., TKK, E-TEK)[12] is also plotted in the figure. As clearly shown, the D-Pt_4Ni_6 exhibits a 6-fold higher Pt-mass activity compared with that of the commercial Pt/C. Notably, the enhancement factor of the D-Pt_2Ni_8 was estimated to be approximately 10.

To investigate the remarkable ORR enhancement of the APD-Pt_2Ni_8 thin film, nanostructures of the thin films before (i.e., as-prepared APD thin films) and after the dealloying were observed by high-angle annular dark-field scanning transmission electron microscopy (HAADF-STEM); the results are presented in Figure 4. As evident in Figure 4a, the as-prepared APD-Pt_2Ni_8 exhibits several nanometer-sized particles stacked to a thickness of 30 nm on the substrate. In contrast, in the case of the D-Pt_2Ni_8 (after dealloying) (Figure 4b), the STEM image indicates that the thickness of the catalyst layer decreased from 30 to 20 nm, accompanied by a decrease in the average diameter of each nanoparticle from 3 to 2 nm. The voltammograms for the D-Pt_xNi_{1-x} presented in Figure 2a clearly show that the dissolution current of Ni for the Pt_2Ni_8 was much larger than that for the Pt_4Ni_6. Therefore, the potential cycling conditions used in this study induced dissolution of the Ni atoms located not only at the surface but also at the inner region of the APD-prepared Pt_2Ni_8 thin films.

The thin-film catalysts generally exhibited higher ORR specific activity compared to that for commercial Pt/C

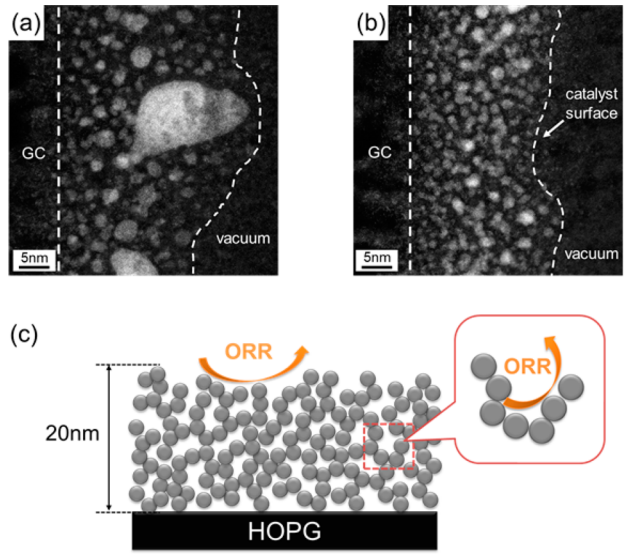

Figure 4. Cross-sectional HAADF-STEM images of Pt_2Ni_8 (as-prepared) (a) and D-Pt_2Ni_8 (dealloyed) (b) on glassy carbon substrates. (c) Schematic of the nanostructure of D-Pt_2Ni_8.

catalysts. For example, Kibsgaard et al. have proposed that the mesostructured Pt thin film with a high surface area exhibits both high ORR activity and durability.[22] Furthermore, Debe and co-workers have reported that Pt−M alloy thin films with an extended flat surface[23] show high specific ORR activity. However, given the practical uses of the alloy thin films as ORR catalysts, the Pt mass activities of the thin-film catalysts (0.1−0.6 A/mg_{-Pt})[22,23] are much lower than that of typical Pt-based alloy NPs (0.6−2.0 A/mg_{-Pt}).[12] Nonetheless, the D-Pt_2Ni_8 thin films with the Pt−Ni nanoparticle-stacking structure exhibit superior Pt mass activity compared with that of recently reported shape-controlled Pt−Ni NPs,[24] except for Pt−Ni nanoframe catalysts demonstrating the current highest mass activity at 0.9 V versus RHE.[25]

The Pt mass activities of Pt−Ni alloy catalysts depend on the alloy compositions.[26−28] Because the alloy composition for both the APD-prepared Pt_4Ni_6 and the Pt_2Ni_8 are almost identical after the dealloying (Pt_7Ni_3), the ligand effect of the Ni might occur to the same degree in both materials. As clearly evident in Figure 4b, the D-Pt_2Ni_8 (NPSTF) exhibits a unique nanostructure that is composed of stacked 2−3 nm-sized Pt−Ni nanoparticles. Therefore, the ORR activity enhancement factor of 10 for the NPSTF D-Pt_2Ni_8 likely originates primarily from the nanostructure composed of effective stacking of the Pt−Ni NPs. A schematic of the NPSTF D-Pt_2Ni_8 structures is depicted in Figure 4c, where 2−3 nm-sized Pt−Ni NPs are stacked through electrochemical dealloying. The increased utilization rate of Pt derived from the specific nanoporous-like structure should lead to extremely high mass activity of the NPSTF D-Pt_2Ni_8.

Finally, the stability test for the D-Pt_2Ni_8 was conducted by applying potential cycling between 0.6 and 1.0 V (Supporting Information Figure S1). After 5000 cycles, although the electrochemical surface area retained 90% of the initial, the Pt mass activity decreased by 45%. The results suggest that potential cycles induced structural changes of the D-Pt_2Ni_8 accompanying with Ni dissolution. However, it is worth nothing that the mass activity after 5000 cycles (0.68 A/mg_{-Pt}) is still higher than the initial activities of the commercial

DOI: 10.1021/acscatal.5b00065
ACS Catal. 2015, 5, 2209−2212

Pt/C[11] and the previously reported Pt-based thin films.[22,23] A systematic study is underway to assess the long-term stability, activity, structure, and composition, during potential cycles.

In this study, we synthesized Pt−Ni thin-film catalysts on HOPG substrates via the synchronous APD of Pt and Ni followed by electrochemical dealloying. The alloy composition for the APD-Pt_4Ni_6 and APD-Pt_2Ni_8 was estimated to be Pt_7Ni_3 after the dealloying process. Although the Pt loading and the Pt−Ni alloy composition after the dealloying were fixed, the Pt-mass activities of the D-Pt_4Ni_6 and D-Pt_2Ni_8 differed substantially: the enhancement factors for the former and latter APD-prepared Pt−Ni thin films compared with typical Pt/C commercial catalysts were 6 and 10. The remarkable activity enhancement of the D-Pt_2Ni_8 was attributed to its unique nanoporous-like structures composed of 2−3 nm-sized Pt−Ni nanoparticles stacked on the HOPG substrate. We hope that the NPSTF structures synthesized in this study will provide a structural basis for the development of highly active and cost-effective ORR catalysts.

■ ASSOCIATED CONTENT

Supporting Information

The following file is available free of charge on the ACS Publications website at DOI: 10.1021/acscatal.5b00065.

Experimental details, results of stability test for the D-Pt_2Ni_8, and selected references (PDF)

■ AUTHOR INFORMATION

Corresponding Author

*Email: n-todoroki@material.tohoku.ac.jp.

Notes

The authors declare no competing financial interest.

■ ACKNOWLEDGMENTS

This study was supported by the New Energy and Industrial Technology Development Organization (NEDO) of Japan.

■ REFERENCES

(1) Paulus, U. A.; Wokaun, A.; Scherer, G. G.; Schmidt, T. J.; Stamenkovic, V.; Markovic, N. M.; Ross, P. N. *Electrochim. Acta* **2002**, *47*, 3787−3798.

(2) Lee, K.-S.; Park, H.-Y.; Ham, H. C.; Yoo, S. J.; Kim, H. J.; Cho, E.; Manthiram, A.; Jang, J. H. *J. Phys. Chem. C* **2013**, *117*, 9164−9170.

(3) Sasaki, K.; Wang, J. X.; Naohara, H.; Marinkovic, N.; More, K.; Inada, H.; Adzic, R. R. *Electrochim. Acta* **2010**, *55*, 2645−2652.

(4) Gan, L.; Heggen, M.; Rudi, S.; Strasser, P. *Nano Lett.* **2012**, *12*, 5423−5430.

(5) Gasteiger, H. A.; Kocha, S. S.; Sompalli, B.; Wagner, F. T. *Appl. Catal., B* **2005**, *56*, 9−35.

(6) Wang, H.; Ishihara, S.; Ariga, K.; Yamauchi, Y. *J. Am. Chem. Soc.* **2012**, *134*, 10819−10821.

(7) Bonakdarpour, A.; Lake, K.; Stevens, K.; Dahn, J. R. *J. Electrochem. Soc.* **2008**, *155*, B108−B118.

(8) Debe, M. K.; Schmoeckel, A. K.; Vernstrom, G. D.; Atanasoski, R. *J. Power Sources* **2006**, *161*, 1002−1011.

(9) van der Vliet, D. F.; Wang, C.; Tripkovic, D.; Strmcnik, D.; Zhang, X. F.; Debe, M. K.; Atanasoski, R. T.; Markovic, N. M.; Stamenkovic, V. R. *Nat. Mater.* **2012**, *11*, 1051−1058.

(10) Henry, J. B.; Maljusch, A.; Huang, M.; Schuhmann, W.; Bondarenko, A. S. *ACS Catal.* **2012**, *2*, 1457−1460.

(11) Hwang, S.-M.; Lee, C. H.; Kim, J. J.; Moffat, T. P. *Electrochim. Acta* **2010**, *55*, 8938−8946.

(12) Debe, M. K. *Nature* **2012**, *486*, 43−51.

(13) Yang, R.; Leisch, J.; Strasser, P.; Toney, M. F. *Chem. Mater.* **2010**, *22*, 4712−4720.

(14) Stamenkovic, V. R.; Mun, B. S.; Mayrhofer, K. J. J.; Ross, P. N.; Markovic, N. M. *J. Am. Chem. Soc.* **2006**, *128*, 8813−8819.

(15) Rudi, S.; Tuaev, X.; Strasser, P. *Electrocatalysis* **2012**, *3*, 265−273.

(16) Lee, S. W.; Chen, S.; Suntivich, J.; Sasaki, K.; Adzic, R. R.; Shao-Horn, Y. *J. Phys. Chem. Lett.* **2010**, *1*, 1316−1320.

(17) Stamenkovic, V. R.; Fowler, B.; Mun, B. S.; Wang, G.; Ross, P. N.; Lucas, C. A.; Markovic, N. M. *Science* **2007**, *315*, 493−497.

(18) Stephens, I. E. L.; Bondarenko, A. S.; Gronbjerg, U.; Rossmeisl, J.; Chorkendorff, I. *Energy Environ. Sci.* **2012**, *5*, 6744−6762.

(19) Todoroki, N.; Asakimori, Y.; Wadayama, T. *Phys. Chem. Chem. Phys.* **2013**, *15*, 17771−17774.

(20) Yamada, Y.; Miyamoto, K.; Hayashi, T.; Iijima, Y.; Todoroki, N.; Wadayama, T. *Surf. Sci.* **2013**, *607*, 54−60.

(21) van der Vliet, D. F.; Wang, C.; Li, D.; Paulikas, A. P.; Greeley, J.; Rankin, R. B.; Strmcnik, D.; Tripkovic, D.; Markovic, N. M.; Stamenkovic. *Angew. Chem.* **2012**, *124*, 3193−3196.

(22) Kibsgaard, J.; Gorlin, Y.; Chen, Z.; Jaramillo, T. F. *J. Am. Chem. Soc.* **2012**, *134*, 7758−7765.

(23) van der Vliet, D.; Wang, C.; Debe, M.; Atanasoski, R.; Markovic, N. M.; Stamenkovic, V. R. *Electrochim. Acta* **2011**, *56*, 8695−8699.

(24) Cui, C.; Gan, L.; Heggen, M.; Rudi, S.; Strasser, P. *Nat. Mater.* **2013**, *12*, 765−771.

(25) Chen, C.; Kang, Y.; Huo, Z.; Zhu, Z.; Huang, W.; Xin, H. L.; Snyder, J. D.; Li, D.; Herron, J. A.; Mavrikakis, M.; Chi, M.; More, K. L.; Li, Y.; Markovic, N. M.; Somorjai, G. A.; Yang, P.; Stamenkovic, V. R. *Science* **2014**, *343*, 1339−1343.

(26) Cui, C.; Gan, L.; Neumann, M.; Heggen, M.; Roldan Cuenya, B.; Strasser, P. *J. Am. Chem. Soc.* **2014**, *136*, 4813−4816.

(27) Liu, Y.; Hangarter, C. M.; Bertocci, U.; Moffat, T. P. *J. Phys. Chem. C* **2012**, *116*, 7848−7862.

(28) Toda, T.; Igarashi, H.; Uchida, H.; Watanabe, M. *J. Electrochem. Soc.* **1999**, *146*, 3750−3756.

DOI: 10.1021/acscatal.5b00065
ACS Catal. 2015, 5, 2209−2212